I&EC research
Industrial & Engineering Chemistry Research

Article

pubs.acs.org/IECR

CO_2 Chemisorption and Cyclability Analyses of Lithium Aluminate Polymorphs (α- and β-Li_5AlO_4)

Tatiana Ávalos-Rendón,[†] Víctor H. Lara,[‡] and Heriberto Pfeiffer*,[†]

[†]Instituto de Investigaciones en Materiales, Universidad Nacional Autónoma de México, Circuito exterior s/n, Ciudad Universitaria, Delegación Coyoacán, CP 04510, México D.F., Mexico

[‡]Departamento de Química, Universidad Autónoma Metropolitan-Iztapalapa, Av. Michoacán y la Purísima, Del. Iztapalapa, C.P. 09340, México D.F., Mexico

ABSTRACT: The α- and β-Li_5AlO_4 polymorphs were synthesized using a solid-state reaction. The polymorphs were then characterized by X-ray diffraction (XRD), X-ray thermodiffraction (XRTD), and N_2 adsorption. To determine the CO_2 chemisorption capacity, the lithium aluminate polymorphs were analyzed thermogravimetrically in the presence of a CO_2 flux. In addition, a cyclability study was performed on these ceramic materials. Although the results appear very similar for the two phases, α-Li_5AlO_4 exhibits a better CO_2 chemisorption performance. The cyclic performance tests indicate that both materials exhibit a gradually reduced chemisorption capacity after multicycle processes. However, even after many cycles, the chemisorption capacity is considerably high in comparison to other lithium ceramics tested as CO_2 absorbents.

1. INTRODUCTION

Carbon dioxide (CO_2) is a major anthropogenic greenhouse gas, which causes global warming and climate change. The rapid increase in Earth's population over the last few decades, combined with an improvement in the quality of life, are directly related to the dramatic increase in the concentration of man-made CO_2, as both are related to the production and consumption of energy primarily obtained from fossil fuels.[1−3] To mitigate the impact of greenhouse gases, it is critical to trap CO_2 from fossil fuel power plants. The first step in carbon sequestration is the CO_2 capture from flue gas.[3−6] To this end, a variety of lithium ceramics have been tested as possible CO_2-capturing materials.[7−48]

Among these ceramics, lithium aluminates ($LiAlO_2$ and β-Li_5AlO_4) were recently tested as possible CO_2-capturing materials.[49] Although $LiAlO_2$ was unable to chemisorb CO_2, β-Li_5AlO_4 is able to capture CO_2 by a mechanism similar to the one reported for other lithium ceramics. Additionally, Li_5AlO_4 appears to be one of the best options as a CO_2-capturing material because of its high theoretical CO_2 chemisorption capacity due to its Li/Al molar ratio of 5 and the fact that aluminum is lighter than any other element tested, including zirconium, copper, and even silicon. The maximum CO_2 chemisorption capacity of β-Li_5AlO_4 is 19.77 mmol/g, assuming that five lithium atoms react with CO_2 to produce Li_2CO_3. It should also be noted that β-Li_5AlO_4 is able to chemisorb CO_2 over a wide range of temperatures (200−700 °C).[49] Therefore, because β-Li_5AlO_4 has the best CO_2 chemisorption capacity per gram among various lithium ceramics, Li_5AlO_4 is an important case of study as a CO_2 chemisorbent.

Two Li_5AlO_4 polymorphs have been identified—the α- and β-Li_5AlO_4—and detailed structural analyses have been performed.[50,51] The low temperature phase (α-Li_5AlO_4) transforms into a high temperature phase (β-Li_5AlO_4) at approximately 780 °C.[52] These structures are ordered derivatives of the antifluorite (Li_2O) structure with vacancies that occupy distinct lattice positions and can be formulated as $Li_5V_2AlO_4$, where V represents a vacancy.[53,54] The α-Li_5AlO_4 phase crystallizes in the orthorhombic space group *Pbca* with a = 9.087, b = 8.947, and c = 9.120 Å, with Z = 8. In contrast, the β-Li_5AlO_4 phase crystallizes in the orthorhombic space group *Pmmn* with a = 6.420, b = 6.302, and c = 4.620 Å, where Z = 2.[50,51] In both polymorphs, the metallic atoms (Li and Al) and the vacancies occupy tetrahedral sites and their ordered arrangement causes an orthorhombic distortion from cubic symmetry.

Therefore, the aim of this paper was to perform the synthesis and characterization of the α- and β-Li_5AlO_4 polymorphs and then a kinetic analysis of the CO_2 chemisorption capacity and cyclability to determine if either of the two phases exhibit better CO_2 chemisorption behavior.

2. EXPERIMENTAL SECTION

The α-Li_5AlO_4 and β-Li_5AlO_4 phases were synthesized using a solid-state reaction that employs lithium oxide (Li_2O, Aldrich) and gamma aluminum oxide (γ-Al_2O_3, Aldrich).[55] Initially, the powders were mechanically mixed and pressed into pellets (2.5 tons/cm^2). Pellets must be used because the synthesis does not produce the desired product when powders are employed. Subsequently, the pellets were heated under different conditions: the α-Li_5AlO_4 pellets were heated to 500 °C for 24 h, while the β-Li_5AlO_4 pellets were heated to 900 °C for 24 h and rapidly cooled to room temperature. Finally, the α- and β-Li_5AlO_4 pellets were pulverized. To obtain pure α- and β-Li_5AlO_4, 30 and 20 wt % excess lithium was used, respectively, due to lithium's tendency to sublimate. The use of excess

Received: July 29, 2011
Revised: January 20, 2012
Accepted: January 20, 2012
Published: January 20, 2012

dx.doi.org/10.1021/ie201616h | *Ind. Eng. Chem. Res.* 2012, 51, 2622−2630

lithium in similar quantities than those mentioned above did not produce the corresponding pure phases.

Two different kinds of XRD measurements were performed: standard X-ray diffraction and X-ray thermodiffraction. In both cases, a diffractometer (Bruker AXS, D8 Advance) coupled to a copper anode X-ray tube was used. The Li_5AlO_4 polymorphs were identified by the corresponding Joint Committee Powder Diffraction Standards (JCPDS). The X-ray thermodiffraction patterns were obtained by scanning from room temperature to 1000 °C, at a temperature step of 100 °C, using a platinum−rhodium holder. In this case, the thermal expansion of the X-ray thermodiffractograms was corrected using Pt peaks as the internal standard. Nitrogen adsorption−desorption isotherms and BET surface area analyses were performed using the Bel-Jpn. Minisorp II instrument at 77 K, using a multipoint technique. Samples were previously degassed at 85 °C for 12 h in vacuum.

Different thermal analyses were performed using a Q500HR instrument from TA Instruments. Initially, a set of samples was dynamically heated from room temperature to 900 at 5 °C/min, using a CO_2 flow rate of 60 mL/min (Praxair, grade 3.0). Subsequently, the Li_5AlO_4 samples were tested isothermically at different temperatures (from 350 to 675 °C) in the presence of the same CO_2 flux. For the isothermal analysis, samples were initially heated to 675 at 100 °C/min with a subsequent isothermal treatment of 60 min, using a N_2 flow. This procedure was conducted to ensure that all the samples received equivalent sintering prior to performing the CO_2 chemisorption isotherms. Each sample was then cooled down to its respective isothermal temperature to perform an independent CO_2 chemisorption process. Once the sample reached the corresponding temperature, the flow gas was switched from N_2 to CO_2 and the isothermal experiments were performed using a gas flow rate of 60 mL/min during the duration of the experiment. The regenerability tests were conducted under the uptake conditions in a CO_2 atmosphere (700 °C for 20 min) and the desorption conditions in a N_2 atmosphere (750 °C for 20 min). A flow rate of 60 mL/min was used for all gases. Finally, to elucidate the mechanism of CO_2 capture by the Li_5AlO_4 polymorphs, some of the products obtained from the thermal analyses were characterized by XRD.

3. RESULTS AND DISCUSSION

3.1. Characterization. Figure 1 presents the XRD patterns of the two lithium aluminate polymorphs. The low temperature

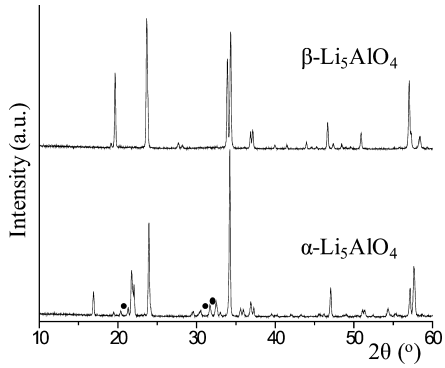

Figure 1. XRD patterns of both of the lithium aluminate polymorph samples. Peaks labeled with this symbol • correspond to Li_2CO_3.

(α-Li_5AlO_4) and the high temperature (β-Li_5AlO_4) phases were synthesized using a solid-state reaction, and the data were fitted with the XDR patterns for 70−2643 and 70−0432 JCPDS files, respectively. Additionally, some small peaks corresponding to lithium carbonate (Li_2CO_3, JCPDS 22-1141) were found in the α-Li_5AlO_4 sample. The Li_2CO_3 was not used as a reagent; thus, it must have been produced during the synthesis due to the use of excess lithium. It should be mentioned that similar amounts of Li_2CO_3 were found in different iterations of α-Li_5AlO_4 synthesis, where the amount of excess lithium varied from 5 to 30% (data not shown). Therefore, it cannot be attributed to the excess lithium in the samples. In the case of β-Li_5AlO_4, there were no other phases detected by XRD, and thus, it could be considered a pure phase, at least according to the detection limit of XRD. Additionally, the surface area of both ceramics was measured using the BET model to be 0.5 and 0.2 m^2/g for the α- and β-Li_5AlO_4 phases, respectively.

To check the thermal stability and transition temperature of the α-Li_5AlO_4 polymorph, a sample was analyzed by thermodiffraction (Figure 2). The XRD patterns did not

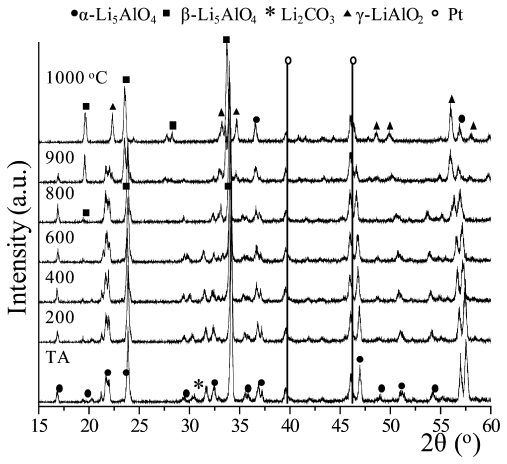

Figure 2. XRD patterns of the α-Li_5AlO_4 sample heated at different temperatures.

exhibit any changes between room temperature and 700 °C. However, when the sample was heated to 800 °C, the lithium carbonate peaks faded away because the melting point of Li_2CO_3 is 720 °C. Additionally, the β-Li_5AlO_4 phase began to appear. This result is in agreement with the α- to β-Li_5AlO_4 phase transition temperature, which is approximately 780 °C. Upon heating to 900 °C, the thermodiffraction pattern exhibited the formation of γ-$LiAlO_2$ (JCPDS 38-1464). The Li_5AlO_4 decomposed to form γ-$LiAlO_2$, which may have occurred via the sublimation of lithium, according to the following reaction 1:[56]

$$Li_5AlO_{4(s)} \rightarrow 4Li_{(g)} + O_{2(g)} + LiAlO_{2(s)} \quad (1)$$

Lithium sublimation has been observed in several lithium ceramics in this temperature range (600−900 °C),[9,57−60] and in this case, the lithium sublimation must be accelerated as the thermodiffraction experiments were performed in a vacuum chamber. As a summary, the α-Li_5AlO_4 phase is stable until 700 °C because, above this temperature, the polymorphic transformation of α- to β-Li_5AlO_4 phase takes place.

3.2. CO_2 Chemisorption. Once the samples were characterized and the thermal stability of the α-Li_5AlO_4 phase

dx.doi.org/10.1021/ie201616h | Ind. Eng. Chem. Res. 2012, 51, 2622−2630

was evaluated, the CO_2 chemisorption capacities of both Li_5AlO_4 polymorphs were analyzed thermogravimetrically in the presence of a CO_2 flux. Figure 3 provides the dynamic

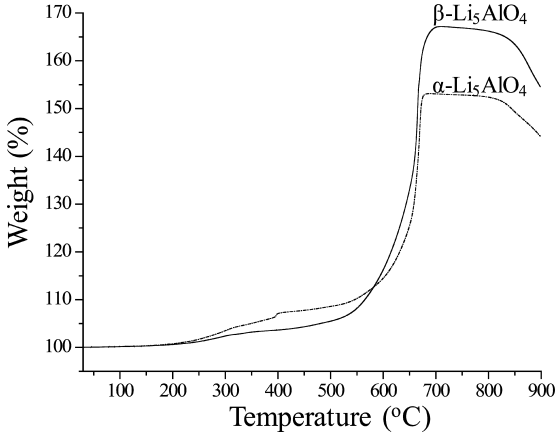

Figure 3. Dynamic thermogram analysis of the both lithium aluminate polymorphs in a CO_2 flow.

thermograms of α-Li_5AlO_4 and β-Li_5AlO_4 in the presence of a CO_2 flux. Both ceramics show similar trends and exhibit very high CO_2 chemisorptions, although via two different processes. The first increment of weight change occurred between 210 and 390 °C, and the second between 510 and 690 °C. These kinds of thermal trends have already been observed for other lithium ceramics.[40,42,49,61,62] For example, recently Li_2CuO_2 was tested as a possible CO_2-capturing material, and the results clearly showed that Li_2CuO_2 is able to chemisorb CO_2 chemically in two similar steps.[43] First, at low temperatures, there is a CO_2 chemisorption over the surface of the ceramic, which suggests the formation of an external shell composed of alkaline carbonate. When the temperature is increased sufficiently, diffusion processes are activated, and the reaction continues through the bulk of the material, completing the CO_2 chemisorption. The diffusion processes indicate not only lithium diffusion but also oxygen diffusion because part of the oxygen present in lithium ceramics becomes part of the lithium carbonate external shell.[75] For the α-Li_5AlO_4 and β-Li_5AlO_4, similar behaviors were observed. The surface reaction took place between 210 and 390 °C. The weight increments observed in this process were 5.42 and 2.88 wt % for the α- and β-Li_5AlO_4, respectively. Subsequently, a weight increment of 6.4 wt % was observed between 390 and 580 °C for the α-Li_5AlO_4 phase, whereas the β-Li_5AlO_4 phase did not exhibit a change in weight. This behavior may be explained by the difference in the surface areas between the two polymorphs, which are 0.5 m^2/g for the α-Li_5AlO_4 and 0.2 m^2/g for the β-Li_5AlO_4. The surface area is an important factor at low temperatures, where the superficial CO_2 chemisorption takes place. At temperatures equal or greater than 510 °C, the α-Li_5AlO_4 and β-Li_5AlO_4 absorbed 53.14% and 67.21% of CO_2, respectively. At this temperature, the lithium diffusion should be activated, and the CO_2 chemisorption process was completed. Finally, at temperatures greater than 680 °C, the samples exhibited a desorption process. Although these results suggest that the β-Li_5AlO_4 phase chemisorbs more CO_2 than the α-Li_5AlO_4, this was only a qualitative analysis. A quantitative study was performed, and the results are described below.

To corroborate the reaction mechanism, the α-Li_5AlO_4 sample obtained after the CO_2 chemisorption process (at 700 °C) was characterized by XRD (Figure 4). As it can be seen in

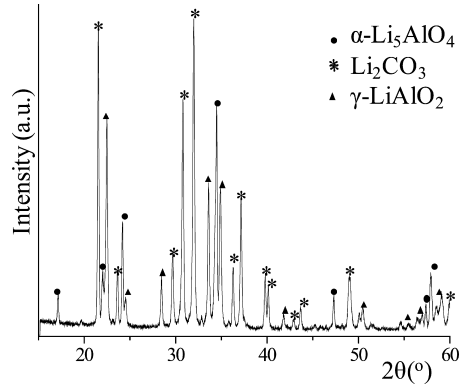

Figure 4. XRD pattern of the α-Li_5AlO_4 sample after the CO_2 chemisorption process.

Figure 4, the XRD pattern was fit with the following JCPDS files: Li_2CO_3 (22-1141), α-Li_5AlO_4 (24-0596), and γ-$LiAlO_2$ (73-1338). These results confirm that the CO_2 is reacting chemically, producing Li_2CO_3 and $LiAlO_2$ as products, independent of the initial phase Li_5AlO_4. Therefore, the correct reaction mechanism between Li_5AlO_4 and CO_2 corresponds to the following reaction 2:

$$Li_5AlO_{4(s)} + 2CO_{2(g)} \rightarrow 2Li_2CO_{3(s)} + LiAlO_{2(s)} \quad (2)$$

For this reaction, the actual Li_5AlO_4 maximum CO_2 chemisorption capacity corresponds to 15.91 mmol/g. This result is in good agreement with the reaction system described by Inoue et al.,[63] which was derived from the phase diagram of the $Li_2O-Al_2O_3$ system.[52]

To further analyze the CO_2 chemisorption in the lithium aluminate polymorphs, different and independent kinetic experiments were performed. However, to eliminate the presence of any sintering effect, all the isotherms were initially heated to 675 at 100 °C/min with a subsequent isothermal treatment of 60 min using an N_2 flow. This procedure was performed to ensure that all samples were sintered in an equivalent manner prior to performing the CO_2 absorption isotherms, eliminating any sintering effect observed in previous works.[49] Each sample was then cooled down to its respective isothermal temperature for the CO_2 chemisorption. Once the sample reached the corresponding temperature, the flow gas was switched from N_2 to CO_2 and the isothermal experiments were performed. The kinetic data was only obtained for the initial CO_2 absorption, to avoid any kind of physical or chemical interference produced on the samples during the cycle processes.

As expected, all of the isothermal experiments followed a typical behavior (Figure 5), wherein the CO_2 chemisorption by both polymorphs increased as a function of temperature in an exponential manner. For the α-Li_5AlO_4 phase (Figure 5A), while the sample that was heated to 600 °C chemisorbed 20.3 wt % of CO_2 after 3.5 h, the total weight increment observed at 675 °C was 41.8 wt % for the same period of time. This means that at 675 °C, the α-Li_5AlO_4 phase is able to chemisorb twice as much CO_2 than at 600 °C. However, the samples heated between 625 and 650 °C increased their weight by only 25 and 26 wt %, respectively. In contrast, the β-Li_5AlO_4 phase (Figure

dx.doi.org/10.1021/ie201616h | Ind. Eng. Chem. Res. 2012, 51, 2622−2630

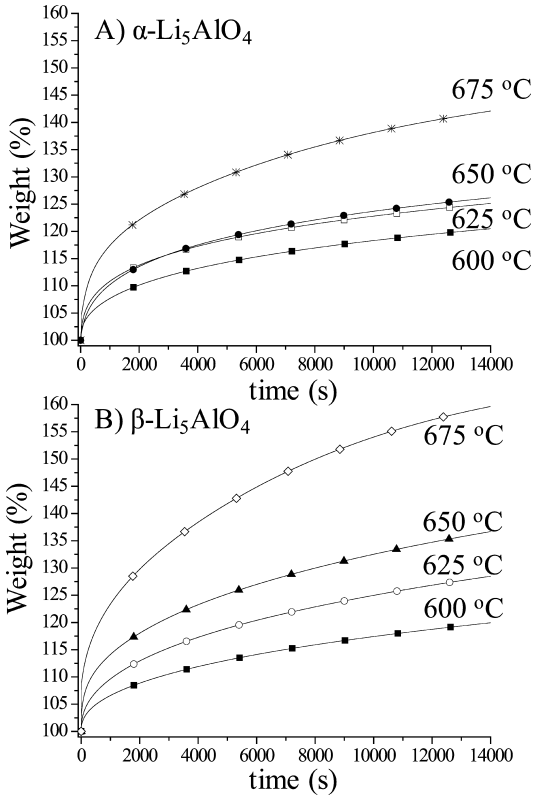

Figure 5. Isotherms of CO_2 chemisorption on both lithium aluminate polymorphs at different temperatures after a sintering process at 675 °C.

5B) showed that the amount of CO_2 chemisorbed increased dramatically as a function of temperature. Therefore, in the isothermal analyses at 600, 625, 650, and 675 °C, the weight gain was 20.2, 29.3, 37.4, and 59.4 wt %, respectively. This indicates that at 675 °C, the β-Li_5AlO_4 phase is able to chemisorb three times more CO_2 than at 600 °C. None of the isothermal analyses reached the plateau. The diffusion processes at this temperature appears to be slow for this polymorph. However, at 675 °C, the diffusion process is completely activated, and the surface area is not a critical factor. Additionally, at longer times, the maximum CO_2 chemisorption capacity increased in both polymorphs because at longer periods, the weight increment depends on the diffusion processes, which are activated at higher temperatures.

After the qualitative analysis of the isothermal experiments, the curves were fit to a double exponential model (eq 3) because it has been reported that two different processes take place: CO_2 chemisorption over the Li_5AlO_4 surface of the particles (*process 1*), which indicates the formation of an external shell of alkaline carbonate, and the CO_2 chemisorption kinetically controlled by diffusion processes (*process 2*).[49] The double exponential model to which the isotherms were fit is defined by the following equation:

$$y = A\exp^{-k_1 t} + B\exp^{-k_2 t} + C \quad (3)$$

where y represents the weight percentage of CO_2 chemisorbed, t is the time, and k_1 and k_2 are the exponential constants for the CO_2 chemisorption over the surface of the Li_5AlO_4 particles and the CO_2 chemisorption kinetically controlled by diffusion processes, respectively. Additionally, the pre-exponential factors A and B indicate the intervals during which each process controls the whole CO_2 capture process, and the C constant indicates the y-intercept. The kinetics parameters, pre-exponential constants and R^2 values obtained at each temperature are presented in Table 1.

These results demonstrate that the direct CO_2 chemisorption constant values (k_1) are at least one order of magnitude higher than the CO_2 chemisorption kinetically controlled by diffusion processes constant values (k_2). Additionally, the value of the B constants is always greater than that of the A constants. This means that the CO_2 chemisorption kinetically controlled by diffusion processes occurs during a larger interval of time than the CO_2 chemisorption produced directly over the surface of the particles. This behavior is explained by the fact that the CO_2 chemisorption occurs initially over the surface of the particles, but the majority of the Li_5AlO_4 content is in the bulk of the ceramic, which necessitates the diffusion process. Finally, the constant values k_1 were not very different for the α- and β-Li_5AlO_4 polymorphs. However, the constant values k_2 for the β-Li_5AlO_4 phase were lower by at least one order of magnitude than the constant values k_2 for the α-Li_5AlO_4 phase, which indicates that the diffusion processes are more limited in the β-Li_5AlO_4 phase. Finally, all these results indicate that the rate-limiting step in the total process is the CO_2 chemisorption kinetically controlled by diffusion processes.

To quantitatively analyze these results and the temperature dependence of the different processes, the k_1 and k_2 constant values were fit to Eyring's model (eq 4), which is typically used on heterogeneous reactions and is a solid−gas system reaction in this case:

$$\ln(k_i/T) = -(\Delta H^{\ddagger}/R)(1/T) + \ln E + \Delta S^{\ddagger}/R \quad (4)$$

k_i is the rate constant value of the process i; E is the pre-exponential factor, which in Eyring's formulation is equal to the ratio between the Boltzmann and Planck constants; R is the

Table 1. Kinetic Parameters of the α-Li_5AlO_4 and β-Li_5AlO_4 Isotherms Fitted to a Double Exponential Model

T (°C)	A	B	C	k_1 ($1/s^{-1}$)	k_2 (s^{-1})	R^2
			α			
600	−5.226	−17.120	124.6	1.30×10^{-3}	1.00×10^{-4}	0.99955
625	−7.796	−18.284	128.6	1.81×10^{-3}	1.20×10^{-4}	0.99879
650	−7.949	−20.065	129.8	1.54×10^{-3}	1.20×10^{-4}	0.99949
675	−11.364	−32.781	148.0	2.22×10^{-3}	1.20×10^{-4}	0.99943
			β			
600	−4.368	−19.773	126.0	1.26×10^{-3}	8.00×10^{-5}	0.99967
625	−6.541	−27.382	136.7	1.22×10^{-3}	9.00×10^{-5}	0.99966
650	−8.090	−32.216	145.2	1.61×10^{-3}	9.00×10^{-5}	0.99936
675	−10.255	−49.258	168.4	2.15×10^{-3}	1.20×10^{-4}	0.99969

dx.doi.org/10.1021/ie201616h | *Ind. Eng. Chem. Res.* 2012, 51, 2622−2630

ideal gas constant; and $\Delta H^{\ddagger}$ and $\Delta S^{\ddagger}$ are the activation enthalpy and entropy, respectively. The data demonstrate that $\ln(k/T)$ versus $1/T$ plots can be described by a linear trend when using Eyring's model (Figure 6). Therefore, by fitting the

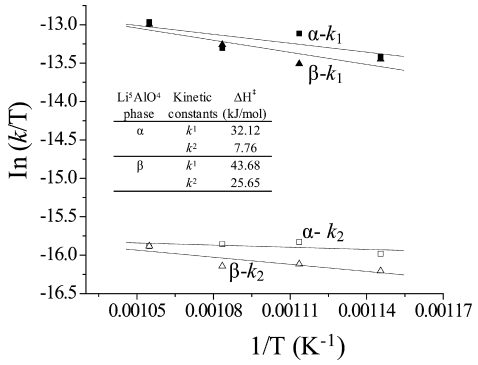

Figure 6. Eyring's plots for the rate constants values of the CO_2 direct chemisorption (k_1), and the CO_2 chemisorption kinetically controlled by diffusion processes (k_2).

data to a linear model, the activation enthalpies ($\Delta H^{\ddagger}$) for the two different processes were calculated (see inset table of Figure 6). The $\Delta H^{\ddagger}$ values obtained for the α-Li_5AlO_4 phase were 32.12 kJ/mol for direct CO_2 chemisorption and 7.76 kJ/mol for CO_2 chemisorption kinetically controlled by diffusion processes. For the β-Li_5AlO_4 polymorph, the $\Delta H^{\ddagger}$ values obtained were 43.68 and 25.65 kJ/mol for the direct CO_2 chemisorption and the CO_2 chemisorption kinetically controlled by diffusion processes, respectively. These results confirm that in both polymorphs, the CO_2 direct chemisorption process is more dependent on the temperature than the CO_2 chemisorption kinetically controlled by diffusion processes, at least in the temperature range of 600−675 °C. In other words, while the CO_2 direct chemisorption is considerably improved as a function of the temperature, the CO_2 chemisorption controlled by diffusion processes does not change significantly, which is inline with the k_2 constant values reported in Table 1. In a previous paper,[49] the $\Delta H^{\ddagger}$ values obtained indicated that the CO_2 chemisorption controlled by diffusion processes was more dependent on the temperature than CO_2 direct chemisorption. However, in that case, the $\Delta H^{\ddagger}$ values were calculated from a considerably larger temperature range (300−675 °C). Nevertheless, the k_2 constant values were varied by two orders of magnitude between 300 and 675 °C, but the values obtained, between 600 and 675 °C, are very similar to those obtained in this work. Therefore, the variations observed between these works must correspond to the temperature range taken into account in each case, wherein the $\Delta H^{\ddagger}$ calculation is very sensitive to this parameter.

3.3. CO_2 Cyclability. To assess the regeneration properties and the thermal stability after several cycles of CO_2 chemisorption/desorption in both lithium aluminate polymorphs, the samples were tested using a multicycle method. Figure 7 shows the CO_2 chemisorption/desorption multicycle performance of the α- and β-Li_5AlO_4 polymorphs. The result for the α-Li_5AlO_4 phase (dotted line) indicates that the CO_2 chemisorption capacity reaches approximately 47.7 wt % for the first cycle, and after 20 cycles, the CO_2 chemisorption capacity decreases to 22.1 wt %. For the β-Li_5AlO_4 phase (solid line), the CO_2 chemisorption in the first cycle was 62.3 wt %, but after 20 cycles, its capacity decreased dramatically to only 8.1 wt

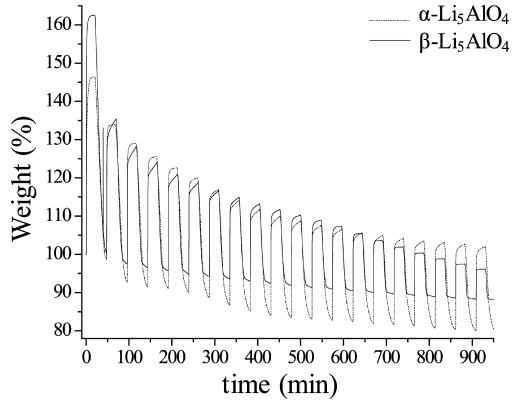

Figure 7. Multicycle performance of CO_2 chemisorption/desorption on both lithium aluminate polymorphs. CO_2 absorptions were performed at 700 °C for 20 min, while the desorption processes were performed at 750 °C over 20 min into a N_2 flux.

%. Both polymorphs showed a similar behavior during the performance of several cycles. The CO_2 chemisorption decreased gradually after each cycle, and the achieved chemisorption capacity for the corresponding cycle subsequently reduced. The reduced capacity during the multicycle process may be caused by the following: as it can be seen in Figure 7, a fraction of the weight of the absorbent is lost during the multicycle process, perhaps by the sublimation of Li_2O during the desorption process, resulting in a reduction in the CO_2 chemisorption capacity. The α-Li_5AlO_4 phase showed a higher Li_2O sublimation of the two polymorphs because this phase is known to be stable at low temperatures. In contrast, the β-Li_5AlO_4 phase can exist at high temperatures. Additionally, we note that the CO_2 capture capacity in the α-Li_5AlO_4 phase is higher than that of the β-Li_5AlO_4 phase.

To understand the cyclability and the regeneration processes in the α-Li_5AlO_4 phase, a sample obtained after one CO_2 chemisorption/desorption cycle was characterized by XRD (Figure 8). The α-Li_5AlO_4 phases could be identified in the

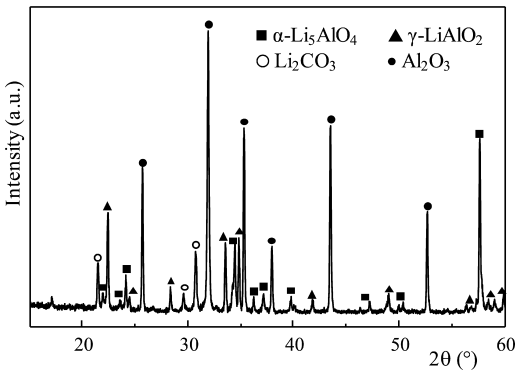

Figure 8. XRD pattern of the α-Li_5AlO_4 sample after the CO_2 cyclic chemisorption process.

XRD patterns, as well as the Li_2CO_3, γ-$LiAlO_2$, and Al_2O_3 phases. These data indicate that the α-Li_5AlO_4 did not exhibit any phase transformation during the cycling experiments. The presence of Al_2O_3 must be attributed to the diffraction generated by the support. Additionally, lithium carbonate cannot correspond to the compound produced during carbonation, as the desorption took place in N_2, which indicates that the ceramic highly reacts with the environmental

dx.doi.org/10.1021/ie201616h | Ind. Eng. Chem. Res. 2012, 51, 2622−2630

Table 2. CO_2 Cyclic Results Obtained on Different Lithium Ceramic

sample	chemisorption temperature (°C)	desorption temperature (°C)	number of cycles	first CO_2 absorption (mmol/g)	last CO_2 absorption (mmol/g)	ref
Li_4SiO_4	700	850	5	2.5	2.5	70
Li_4SiO_4	600	800	50	1.93	1.65	64
Li_4SiO_4	650	750	5	1.91	2.1	33
Li_4SiO_4 (dry milled sample)	740	820	6	2.5	2.5	21
Li_4SiO_4 (wet milled sample)	740	820	10	2.08	1.25	21
Li_4SiO_4 + 2 wt % Li_2ZrO_3	600	800	50	1.98	1.77	64
Li_4SiO_4 + 5 wt % Li_2ZrO_3	600	800	50	2.28	2.14	64
$Li_{3.7}Fe_{0.1}SiO_4$	650	750	5	1.91	1.16	33
Li_4SiO_4 + 20 mol % K_2CO_3	600	600	10	4.54	4.54	71
Li_4SiO_4-based sorbents from fly ash-1 + 40 mol % K_2CO_3	600	600	10	2.27	2.27	71
Li_4SiO_4-based sorbents from fly ash-2 + 40 mol % K_2CO_3	600	600	5	1.36	1.36	71
Li_4SiO_4-based sorbents from fly ash-3 + 40 mol % K_2CO_3	600	600	5	1.31	0.88	71
Li_4SiO_4-qK (crystalline quartz + 10% mol K_2CO_3)	580	800	4	5	5.22	72
Li_2ZrO_3	650	650	8	1.5	1.82	19
Li_2ZrO_3	575	690	11	4.4	4.8	74
Li_2ZrO_3	500	650	3	1.63	1.63	66
Li_2ZrO_3 (Li_2CO_3/K_2CO_3-doped)	550	800	6	1.3	1.3	65
$Li_{2.2}ZrO_{3.1}$	630	630	8	1.3	1.5	20
$K_{0.2}Li_2ZrO_{3.1}$	630	630	8	1.17	1.27	20
$K_{0.2}Li_{1.6}ZrO_{2.9}$	630	630	8	1.18	1.17	20
$K_{0.6}Li_{2.2}ZrO_{3.4}$	630	630	8	1.17	0.65	20
$K_{0.8}Li_{2.2}ZrO_{3.7}$	630	630	8	0.84	0.45	20
91.3% Li_2ZrO_3 + 3.4% Y_2O_3 + 0.2% Al_2O_3 + 5.1% K_2O	500	750	5	1.56	1.37	68
$Li_6Zr_2O_7$	750	850	3	0.38	0.26	67
$Li_6Zr_2O_7$	750	850	7	0.31	0.22	69
Li_8ZrO_6	750	850	4	3.6	2.41	67
Li_8ZrO_6	750	860	11	5.04	2.05	73
α-Li_5AlO_4	700	750	20	9.44	4.38	-
β-Li_5AlO_4	700	750	20	12.33	1.6	-

CO_2. Therefore, after one cycle, Li_2O is still found on the surface of the ceramic, and the ceramic is able to chemisorb CO_2 from the environment.

Table 2 summarizes the cyclability conditions for the different lithium ceramics reported in the literature, although there are other kinetic factors that must be taken into account to establish the best CO_2 absorption conditions for lithium ceramics. Figure 9 compares some of the cyclic stabilities reported for the following lithium ceramics: Li_4SiO_4, Li_2ZrO_3, $Li_6Zr_2O_7$, Li_8ZrO_6, and Li_5AlO_4 (results obtained in this work). As it can be seen from Table 2, most of these ceramics exhibit low CO_2 chemisorption capacities (between 0.4 and 4 mmol/g). However, both lithium aluminates polymorphs exhibit the highest CO_2 chemisorption capacities in a multicycle test. The α- and β-Li_5AlO_4 phases seem to have some of the best cyclic CO_2 chemisorption/desorption behaviors, even compared to other lithium ceramics reported in the literature that were K-doped, which increases the CO_2 chemisorption properties. Therefore, if the lithium aluminates were K-doped, it would increase the CO_2 chemisorption rate because Li_2CO_3 forms a eutectic phase with the K_2CO_3 at high temperatures, resulting in a liquid shell that facilitates the diffusion of CO_2 throughout the product layer.[71,72]

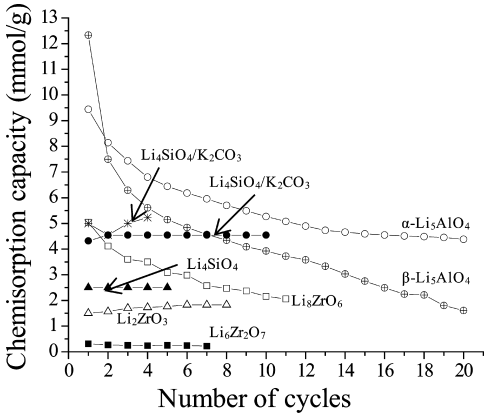

Figure 9. Cyclic stability of different lithium ceramics reported in the literature.[19,69−71,73]

4. CONCLUSIONS

The α- and β-Li_5AlO_4 polymorphs were synthesized using a solid-state reaction and then characterized by XRD and BET. The results indicate that the α-Li_5AlO_4 phase is stable until 700 °C, and above this temperature, the polymorphic transformation into the β-Li_5AlO_4 phase takes place. During the dynamic thermal analyses, both polymorphs showed similar trends and exhibited very high CO_2 chemisorptions. Both

dx.doi.org/10.1021/ie201616h | Ind. Eng. Chem. Res. 2012, 51, 2622−2630

lithium aluminate polymorphs are able to chemisorb CO_2 in a wide temperature range, from 210 to 690 °C, but the α-Li_5AlO_4 phase only chemisorbed 53.14 wt %, whereas the β-Li_5AlO_4 phase chemisorbed 67.21 wt %. As it has been mentioned in previous papers, powder lithium ceramics tend to sinter, which produces an important decrease in the surface area, reducing the CO_2 chemisorption. To avoid the sintering effect and to perform a correct kinetic analysis, samples were homogeneously sintered prior to performing the isothermal experiments. All isotherms were fit to a double exponential model because it can describe two different processes: (1) the CO_2 chemisorption over the surface of the Li_5AlO_4 particles and (2) the CO_2 chemisorption kinetically controlled by diffusion processes. The kinetic constant values indicated that the CO_2 chemisorption kinetically controlled by diffusion processes is the rate-limiting step for the whole process. Additionally, by fitting these data to Eyring's model, the $\Delta H^{\ddagger}$ values were obtained that indicate that the CO_2 direct chemisorption process is more dependent on temperature than the CO_2 chemisorption kinetically controlled by diffusion processes, at least between 600 and 675 °C. The cyclic performance tests indicate that both lithium aluminates polymorphs exhibit a gradually reduced chemisorption capacity during the multicycle processes, perhaps due to the sublimation of the Li_2O during the desorption process, resulting in a reduction in the CO_2 chemisorption capacity. The CO_2 chemisorption capacity in the α-Li_5AlO_4 phase is higher than that of the β-Li_5AlO_4 phase after 20 cycles. Finally, the α- and β-Li_5AlO_4 phases appear to have some of the best cyclic CO_2 chemisorption/desorption behaviors, even compared to other lithium ceramics that have been K-doped, increasing their CO_2 chemisorption efficiencies.

AUTHOR INFORMATION

Corresponding Author

*Member of the ACS. Phone: +52 (55) 56224627. Fax: +52 (55) 56161371. E-mail: pfeiffer@iim.unam.mx.

Notes

The authors declare no competing financial interest.

ACKNOWLEDGMENTS

This work was financially supported by PAPIIT-UNAM (IN100609) and CONACYT-SENER (150358). T.Á.-R. thanks CONACYT for personal financial supports. The authors would like to thanks to A. Tejeda for technical help.

REFERENCES

(1) Reddy, E. P.; Smirniotis, P. G. High-Temperature Sorbents for CO_2 Made of Alkali Metals Doped on CaO Supports. *J. Phys. Chem. B.* **2004**, *108*, 7794.

(2) Lee, K. B.; Beaver, M. G.; Caram, H. S.; Sircar, S. Reversible Chemisorbents for Carbon Dioxide and their Potential Applications. *Ind. Eng. Chem. Res.* **2008**, *47*, 8048.

(3) Schrag, D. P. Confronting the Climate-Energy Challenge. *Elements* **2007**, *3*, 171.

(4) Friedmann, S. J. Geological Carbon Dioxide Sequestration. *Elements* **2007**, *3*, 179.

(5) Busch, A.; Alles, S.; Gensterblum, Y.; Prinz, D.; Dewhurst, D. N.; Raven, M. D.; Stanjek, H.; Krooss, B. M. Carbon Dioxide Storage Potential of Shales. *Inter J. Greenhouse Gas Control* **2008**, *2*, 297.

(6) Leuning, R.; Etheridge, D.; Luhar, A.; Dunse, B. Atmospheric Monitoring and Verification Technologies for CO_2 Geosequestration. *Inter. J. Greenhouse Gas Control* **2008**, *2*, 401.

(7) Xiong, R.; Ida, J.; Lin, Y. S. Kinetics of Carbon Dioxide Sorption on Potassium-Doped Lithium Zirconate. *Chem. Eng. Sci.* **2003**, *58*, 4377.

(8) Olivares-Marín, M.; Castro-Díaz, M.; Drage, T. C.; Maroto-Valerand, M. M. Use of Small-Amplitude Oscillatory Shear Rheometry to Study the Flow Properties of Pure and Potassium-Doped Li_2ZrO_3 Sorbents during the Sorption of CO_2 at High Temperatures. *Sep. Purif. Technol.* **2010**, *73*, 415.

(9) Pfeiffer, H.; Bosch, P. Thermal Stability and High-Temperature Carbon Dioxide Sorption on Hexa-Lithium Zirconate ($Li_6Zr_2O_7$). *Chem. Mater.* **2005**, *17*, 1704.

(10) Ida, J.; Xiong, R.; Lin, Y. S. Synthesis and CO_2 Sorption Properties of Pure and Modified Lithium Zirconate. *Sep. Purif. Technol.* **2004**, *36*, 41.

(11) Nakagawa, K.; Ohashi, T. A Reversible Change between Lithium Zirconate and Zirconia in Molten Carbonate. *Electrochemistry* **1999**, *67*, 618.

(12) Fauth, D. J.; Frommell, E. A.; Hoffman, J. S.; Reasbeck, R. P.; Pennline, H. W. Eutectic Salt Promoted Lithium Zirconate: Novel High Temperature Sorbent for CO_2 Capture. *Fuel Process. Technol.* **2005**, *86*, 1503.

(13) Choi, K. H.; Korai, Y.; Mochida, I. Preparation of CO_2 Absorbent by Spray Pyrolysis. *Chem. Lett.* **2003**, *32*, 924.

(14) Hwang, K. S.; Lee, Y. H.; Hwangbo, S. Preparation of Lithium Zirconate Nanopowder Prepared by Electrostatic Spraying for CO_2 Sorbent. *Mater. Sci. Poland* **2007**, *25*, 969.

(15) Nair, B. N.; Yamaguchi, T.; Kawamura, H. Processing of Lithium Zirconate for Applications in Carbon Dioxide Separation: Structure and Properties of the Powders. *J. Am. Ceram. Soc.* **2004**, *87*, 68.

(16) Yi, K. B.; Eriksen, D. Ø. Low Temperature Liquid State Synthesis of Lithium Zirconate and its Characteristics as a CO_2 Sorbent. *Sep. Sci. Technol.* **2006**, *41*, 283.

(17) Duan, Y. Electronic Structural and Electrochemical Properties of Lithium Zirconates and their Capabilities of CO_2 Capture: A First-Principles Density-Functional Theory and Phonon Dynamics Approach. *J. Renewable Sustainable Energy* **2011**, *3*, 013102.

(18) Duan, Y.; Zhang, B.; Sorescu, D. C.; Johnson, J. K. CO_2 Capture Properties of M−C−O−H (M = Li, Na, K) Systems: A Combined Density Functional Theory and Lattice Phonon Dynamics Study. *J. Solid State Chem.* **2011**, *184*, 311.

(19) Kang, S. Z.; Wu, T.; Li, X.; Mu, J. Low Temperature Biomimetic Synthesis of the Li_2ZrO_3 Nanoparticles Containing $Li_6Zr_2O_7$ and High Temperature CO_2 Capture. *Mater. Lett.* **2010**, *64*, 1404.

(20) Ochoa-Fernández, E.; Rønning, M.; Yu, X.; Grande, T.; Chen, D. Compositional Effects of Nanocrystalline Lithium Zirconate on its CO_2 Capture Properties. *Ind. Eng. Chem. Res.* **2008**, *47*, 434.

(21) Nair, B. N.; Burwood, R. P.; Goh, V. J.; Nakagawa, K.; Yamaguchi, T. Lithium Based Ceramic Materials and Membranes for High Temperature CO_2 Separation. *Prog. Mater. Sci.* **2009**, *54*, 511.

(22) Venegas, M. J.; Fregoso-Israel, E.; Pfeiffer, H. Kinetic and Reaction Mechanism of CO_2 Sorption on Li_4SiO_4: Study of the Particle Size Effect. *Ind. Eng. Chem. Res.* **2007**, *46*, 2407.

(23) Okumura, T.; Enomoto, K.; Togashi, N.; Oh-ishi, K. CO_2 Absorption Reaction of Li_4SiO_4 Studied by the Rate Theory using Thermogravimetry. *J. Ceram. Soc. Jpn.* **2007**, *115*, 491.

(24) Escobedo-Bretado, M.; Guzmán-Velderrain, V.; Lardizabal-Gutierrez, D. New Synthesis Route to Li_4SiO_4 as CO_2 Catalytic/Sorbent. *Catal. Today* **2005**, *107*, 863.

(25) Essaki, K.; Nakagawa, K.; Kato, M.; Uemoto, H. CO_2 Absorption by Lithium Silicate at Room Temperature. *J. Chem. Eng. Jpn.* **2004**, *37*, 772.

(26) Essaki, K.; Kato, M.; Uemoto, H. Influence of Temperature and CO_2 Concentration on the CO_2 Absorption Properties of Lithium Silicate Pellets. *J. Mater. Sci.* **2005**, *18*, 5017.

(27) Khomane, R. B.; Sharma, B.; Saha, S.; Kulkarni, B. D. Reverse Microemulsion Mediated Sol−Gel Synthesis of Lithium Silicate Nanoparticles under Ambient Conditions: Scope for CO_2 Sequestration. *Chem. Eng. Sci.* **2006**, *61*, 3415.

(28) Wang, K.; Guo, X.; Zhao, P.; Wang, F.; Zheng, C. High Temperature Capture of CO_2 on Lithium-Based Sorbents from Rice Husk Ash. *J. Haz. Mater.* **2011**, *189*, 307.
(29) Rodríguez-Mosqueda, R.; Pfeiffer, H. Thermokinetic Analysis of the CO_2 Chemisorption on Li_4SiO_4 by using Different Gas Flow Rates and Particle Sizes. *J. Phys. Chem. A* **2010**, *114*, 4535.
(30) Kato, M.; Maezawa, Y.; Takeda, S.; Hagiwara, Y.; Kogo, R.; Semba, K.; Hamamura, M. Pre-combustion CO_2 Capture using Ceramic Absorbent and Methane Steam Reforming. *Key Eng. Mater.* **2006**, *317*, 81.
(31) Kato, M.; Yoshikawa, S.; Nakagawa, K. Carbon Dioxide Absorption by Lithium Orthosilicate in a Wide Range of Temperature and Carbon Dioxide Concentrations. *J. Mater. Sci. Lett.* **2002**, *21*, 485.
(32) Tsumura, N.; Kuramoto, A.; Shimamoto, Y.; Aono, H.; Sadaoka, Y. Thermal Stability of Sodium Aluminum Silicates with Alkali Carbonates. *J. Ceram. Soc. Jpn.* **2005**, *113*, 269.
(33) Gauer, C.; Heschel, W. Doped Lithium Orthosilicate for Absorption of Carbon Dioxide. *J. Mater. Sci.* **2006**, *41*, 2405.
(34) Korake, P. V.; Gaikwad, A. G. Capture of Carbon Dioxide over Porous Solid Adsorbents Lithium Silicate, Lithium Aluminate and Magnesium Aluminate at Pre-combustion Temperatures. *Front. Chem. Eng. China* **2011**, *5*, 215.
(35) Yamaguchi, T.; Niitsuma, T.; Nair, B. N.; Nakagawa, K. Lithium Silicate Based Membranes for High Temperature CO_2 Separation. *J. Membr. Sci.* **2007**, *294*, 16.
(36) Kalinkin, A. M.; Kalinkina, E. V.; Zalkind, O. A.; Makarova, T. I. Mechanochemical Interaction of Alkali Metal Metasilicates with Carbon Dioxide: 1. Absorption of CO_2 and Phase Formation. *Colloid J.* **2008**, *70*, 33.
(37) Kalinkin, A. M.; Kalinkina, E. V.; Zalkind, O. A. Mechanochemical Interaction of Alkali Metal Metasilicates with Carbon Dioxide: 2. the Influence of Thermal Treatment on the Properties of Activated Samples. *Colloid J.* **2008**, *70*, 42.
(38) Mejía-Trejo, V. L.; Fregoso-Israel, E.; Pfeiffer, H. Textural, Structural and CO_2 Chemisorption Effects Produced on the Lithium Orthosilicate by its Doping with Sodium ($Li_{4-x}Na_xSiO_4$). *Chem. Mater.* **2008**, *20*, 7171.
(39) López-Ortiz, A.; Perez-Rivera, N. G.; Reyes, A.; Lardizabal-Gutierrez, D. Novel Carbon Dioxide Solid Acceptors using Sodium Containing Oxides. *Sep. Sci. Technol.* **2004**, *39*, 3559.
(40) Alcérreca-Corte, I.; Fregoso-Israel, E.; Pfeiffer, H. CO_2 Absorption on Na_2ZrO_3: A Kinetic Analysis of the Chemisorption and Diffusion Processes. *J. Phys. Chem. C* **2008**, *112*, 6520.
(41) Ueda, S.; Inoue, R.; Sasaki, K.; Wakuta, K.; Ariyama, T. CO_2 Absorption and Desorption Abilities of Li_2O-TiO_2 Compounds. *ISIJ Inter.* **2011**, *51*, 530.
(42) Palacios-Romero, L. M.; Pfeifer, H. Lithium Cuprate (Li_2CuO_2): A new Possible Ceramic Material for CO_2 Chemisorption. *Chem. Lett.* **2008**, *37*, 862.
(43) Palacios-Romero, L. M.; Lima, E.; Pfeifer, H. Structural Analysis and CO_2 Chemisorption Study on non-Stoichiometric Lithium Cuprates ($Li_{2+x}CuO_{2+x/2}$). *J. Phys. Chem. A* **2009**, *113*, 193.
(44) Kato, M.; Essaki, K.; Nakagawa, K.; Suyama, Y.; Terasaka, K. CO_2 Absorption Properties of Lithium Ferrite for Application as a High-Temperature CO_2 Absorbent. *J. Ceram. Soc. Jpn.* **2005**, *113*, 684.
(45) Togashi, N.; Okumura, T.; Oh-Ishi, K. Synthesis and CO_2 Absorption Property of Li_4TiO_4 as a Novel CO_2 Absorbent. *J. Ceram. Soc. Jpn.* **2007**, *115*, 324.
(46) Choi, S.; Drese, J. H.; Jones, C. W. Adsorbent Materials for Carbon Dioxide Capture from Large Anthropogenic Point Sources. *ChemSusChem* **2009**, *2*, 796.
(47) D'Alessandro, D. M.; Smit, B.; Long, J. R. Carbon Dioxide Capture: Prospects for New Materials. *Angew. Chem.* **2010**, *49*, 2.
(48) Pfeiffer, H. Advances in CO_2 Conversion and Utilization. In *ACS Symposium Series*, Hu, Y. H., Ed.; American Chemical Society: Washington, DC, 2010; Vol. *1056*, p 233.
(49) Ávalos-Rendón, T.; Casa-Madrid, J.; Pfeiffer, H. Thermochemical Capture of Carbon Dioxide on Lithium Aluminates ($LiAlO_2$ and Li_5AlO_4): A New Option for the CO_2 Absorption. *J. Phys. Chem. A* **2009**, *113*, 6919.
(50) Stewner, F.; Hoppe, R. Zur Kristallstruktur von α-Li_5AlO_4. *Anorg. Allg. Chem.* **1971**, *380*, 241.
(51) Stewner, F.; Hoppe, R. Zur Kristallstruktur von β-Li_5AlO_4. *Anorg. Allg. Chem.* **1971**, *381*, 149.
(52) Cook, L. P.; Plante, E. R. Phase Diagram of the System Lithia-Alumina. *Ceram. Trans.* **1992**, *27*, 193.
(53) Follstaedt, D. M.; Biefeld, R. M. Nuclear-Magnetic-Resonance Study of Li^+ Motion in Lithium Aluminates and LiOH. *Phys. Rev. B* **1978**, *18*, 5928.
(54) Raistrick, I. D.; Ho, C.; Huggins, R. A. Lithium Ion Conduction in Li_5AlO_4, Li_5GaO_4 and Li_6ZnO_4. *Mater. Res. Bull.* **1976**, *11*, 953.
(55) La-Ginestra, A.; Lo-Jacono, M.; Porta, P. The Preparation, Characterization, and Thermal Behavior of some Lithium Aluminum Oxides: Li_3AlO_3 and Li_5AlO_4. *J. Therm. Anal. Calorim.* **1972**, *4*, 5.
(56) Kulkarni, N. S.; Besmann, T. M.; Spear, K. E. Thermodynamic Optimization of Lithia–Alumina. *J. Am. Ceram. Soc.* **2008**, *91*, 4074.
(57) Pfeiffer, H.; Knowles, K. M. Reaction Mechanisms and Kinetics of the Synthesis and Decomposition of Lithium Metazirconate through Solid-State Reaction. *J. Eur. Ceram. Soc.* **2004**, *24*, 2433.
(58) Cruz, D.; Bulbulian, S.; Lima, E.; Pfeiffer, H. Kinetic Analysis of the Thermal Stability of Lithium Silicates (Li_4SiO_4 and Li_2SiO_3). *J. Solid State Chem.* **2006**, *179*, 909.
(59) Lu, C. H.; Wei-Cheng, L. Reaction Mechanism and Kinetics Analysis of Lithium Nickel Oxide during Solid-State Reaction. *J. Mater. Chem.* **2000**, *10*, 1403.
(60) Antolini, E.; Ferretti, M. Synthesis and Thermal Stability of $LiCoO_2$. *J. Solid State Chem.* **1995**, *117*, 1.
(61) Mosqueda, H.; Vazquez, C.; Bosch, P.; Pfeiffer, H. Chemical Sorption of Carbon Dioxide (CO_2) on Lithium Oxide (Li_2O). *Chem. Mater.* **2006**, *18*, 2307.
(62) Matsukura, Y.; Okumura, T.; Kobayashi, R.; Oh-ishi, K. Synthesis and CO_2 Absorption Properties of Single-Phase Li_2CuO_2 as a CO_2 Absorbent. *Chem. Lett.* **2010**, *39*, 966.
(63) Inoue, R.; Ueda, S.; Wakuta, K.; Sasaki, S.; Ariyama, T. Thermodynamic Consideration on the Absorption Properties of Carbon Dioxide to Basic Oxide. *ISIJ Int.* **2010**, *50*, 1532.
(64) Kato, M.; Nakagawa, K.; Essaki, K.; Maezawa, Y.; Takeda, S.; Kogo, R.; Hagiwara, Y. Novel CO_2 Absorbents using Lithium-Containing Oxide. *Inter. J. Appl. Ceram. Technol.* **2005**, *2*, 467.
(65) Pannocchia, G.; Puccini, M.; Seggiani, M.; Vitolo, S. Experimental and Modeling Studies on High-Temperature Capture of CO_2 using Lithium Zirconate Based Sorbents. *Ind. Eng. Chem. Res.* **2007**, *46*, 6696.
(66) Xiao, Q.; Liu, Y.; Zhong, Y.; Zhu, W. A Citrate Sol–Gel Method to Synthesize Li_2ZrO_3 Nanocrystals with Improved CO_2 Capture Properties. *J. Mater. Chem.* **2011**, *21*, 3838.
(67) Yin, X. S.; Li, S. P.; Zhang, Q. H.; Yu, J. G. Synthesis and CO_2 Adsorption Characteristics of Lithium Zirconates, with High Lithia Content. *J. Am. Ceram. Soc.* **2010**, *93*, 2837.
(68) Iwan, A.; Stephenson, H.; Ketchie, W. C.; Lapkin, A. A. High Temperature Sequestration of CO_2 using Lithium Zirconates. *Chem. Eng. J.* **2009**, *146*, 249.
(69) Yin, X. S.; Li, S. P.; Zhang, Q. H.; Yu, J. G. High-Temperature CO_2 Capture on $Li_6Zr_2O_7$: Experimental and Modeling Studies. *Ind. Eng. Chem. Res.* **2010**, *49*, 6593.
(70) Kato, M.; Nakagawa, K. New Series of Lithium Containing Complex Oxides, Lithium Silicates for Application as a High Temperature CO_2 Absorbent. *J. Ceram. Soc. Jpn.* **2001**, *109*, 911.
(71) Olivares-Marín, M.; Drage, T.C .; Maroto-Valer, M. M. Novel Lithium-Based Sorbents from Fly Ashes for CO_2 Capture at High Temperatures. *Int. J. Greenhouse Gas Control* **2010**, *4*, 623.
(72) Seggiani, M.; Puccini, M.; Vitolo, S.; High-Temperature, S. and Low Concentration CO_2 Sorption on Li_4SiO_4 Based Sorbents: Study of the used Silica and Doping Method Effects. *Int. J. Greenhouse Gas Control* **2011**, *5*, 741.

(73) Yin, X. S.; Zhang, Q. H.; Yu, J. G. Three-Step Calcination Synthesis of High-Purity Li_8ZrO_6 with CO_2 Absorption Properties. *Inorg. Chem.* **2011**, *7*, 2844.
(74) Radfarnia, H. R.; Iliuta, M. C. Surfactant-Template/Ultrasound-Assisted Method for the Preparation of Porous Nanoparticle Lithium Zirconate. *Ind. Eng. Chem. Res.* **2011**, *50*, 9295.
(75) Martínez-dlCruz, L.; Pfeiffer, H. Effect of the Oxygen Addition on the Thermokinetic Properties of CO_2 Chemisorption on Li_2ZrO_3. *Ind. Eng. Chem. Res.* **2010**, *49*, 9038.